Journal of Statistical Physics, Vol. 70, Nos. 1/2, 1993

Stochastic Resonance in Chaotic Dynamics

G. Nicolis,[1] C. Nicolis,[2] and D. McKernan[1]

It is suggested that chaotic dynamical systems characterized by intermittent jumps between two preferred regions of phase space display an enhanced sensitivity to weak periodic forcings through a stochastic resonance-like mechanism. This possibility is illustrated by the study of the residence time distribution in two examples of bimodal chaos: the periodically forced Duffing oscillator and a 1-dimensional map showing intermittent behavior.

KEY WORDS: Stochastic resonance; residence times; bimodal chaos; intermittency.

1. INTRODUCTION

In this paper a class of dynamical systems giving rise to deterministic chaos is identified which exhibit enhanced sensitivity to weak external periodic forcings through a stochastic resonance-like mechanism.

In its classical setting[1-3] stochastic resonance deals with one-variable bistable systems subjected simultaneously to a stochastic forcing and to a weak periodic forcing,

$$\frac{dx}{dt} = -\frac{\partial U}{\partial x} + g(x)(2\mathrm{D})^{1/2} F(t) + \varepsilon h(x) \cos(\omega t + \varphi) \tag{1}$$

where U is a bistable potential; $(2\mathrm{D})^{1/2} F(t)$ is a Gaussian white noise of variance 2D; $g(x)$ and $h(x)$ are coupling terms; and ε, ω, and φ are, respectively, the amplitude, frequency, and phase of the periodic forcing.

As is well known, for

$$\varepsilon \ll 1, \qquad \Delta U/D \gg 1, \qquad \omega \leqslant \tau_{\mathrm{Kr}}^{-1} \tag{2}$$

[1] Faculté des Sciences and Center for Nonlinear Phenomena and Complex Systems, Université Libre de Bruxelles, B-1050 Bruxelles, Belgium.
[2] Institut Royal Météorologique de Belgique, 1180 Bruxelles, Belgium.

0022-4715/93/0100-0125$07.00/0

ΔU and τ_{Kr} being, respectively, the potential barrier and the Kramers time, the response of the variable x to the periodic forcing is enhanced by the presence of noise. Before going to the main subject of the present paper, it is instructive to comment on the origin of this sensitivity. The key point lies in the perturbative solution of the Fokker–Planck equation associated with (1). To the dominant order in ε one finds an expression of the form[4–6] [taking for simplicity $h(x)=1$]

$$\varepsilon \left\langle 1 \left| \frac{\partial}{\partial x} \right| 0 \right\rangle \frac{\lambda_1}{\lambda_1^2+\omega^2} \tag{3}$$

where $|0\rangle$ and $|1\rangle$ are, respectively, the invariant eigenvector and the eigenvector corresponding to the smallest eigenvalue, $\lambda_1 \approx \tau_{\mathrm{Kr}}^{-1}$, of the unperturbed Fokker–Planck operator. Performing the scalar product in (3) using the explicit form of $|0\rangle$, one then finds that the perturbation parameter ε appears through the combination

$$\varepsilon_{\mathrm{eff}} = \frac{\varepsilon}{D} \frac{\lambda_1}{\lambda_1^2+\omega^2} [\text{terms of } O(1)] \tag{4}$$

For D small and under the conditions of (2), λ_1 and ω are also very small and the *effective* ε is thus considerably enhanced. One may understand this enhancement by realizing that a bistable weakly noisy system is in an almost *critical* state, in the sense that the Fokker–Planck operator possesses an eigenvalue λ_1 close to zero. This makes it very sensitive to disturbances of a certain type, such as weak periodic forcings.

As is well known, in many respects deterministic chaos shares the properties of random noise. Recently this idea has been further implemented in discrete-time mappings by showing that, under certain conditions, deterministic chaos can be mapped in an exact manner into a stochastic process governed by a master equation.[7,8] The basic idea is to perform finite coarse-graining by choosing a suitable partition in state space, to project the fine-grained evolution described by the Perron–Frobenius (or Liouville) equation onto the partition, and to require that the evolution of the resulting probability vector be generated by a time-independent transition matrix. One obtains in this way a Chapman–Kolmogorov condition imposing constraints on the partition to be chosen and on the type of dynamical systems amenable to such a description. Alternatively, for dissipative flows for which the above mapping has not yet been carried out in a systematic manner, it has been shown that the evolution may sometimes be cast into a form in which a "deterministic" and an "effective noise" part can be identified.[9,10]

We are now in the position to formulate the main thesis of the present paper: chaotic dynamical systems characterized by intermittent jumps between two preferred regions of phase space should display, on the grounds of the above analogies, an enhanced sensitivity to external periodic forcings through a stochastic resonance-like mechanism. Contrary to systems of the form of Eq. (1), this sensitive response should exist *in the absence of noise*, since chaos generates its own "effective" noise in a spontaneous manner.

In the sequel the validity of this idea will be illustrated on two examples of *bimodal chaos*: the periodically forced Duffing oscillator, and a 1-dimensional map showing intermittent behavior. In each case we first present the main features of the unperturbed system from the standpoint of our main thesis (Sections 2 and 4), and subsequently (Sections 3 and 5) we analyze its response to a weak periodic forcing, with special emphasis on the residence time statistics. The main conclusions are drawn in Section 6.

2. EXAMPLE OF BIMODAL CHAOS: THE PERIODICALLY FORCED DUFFING OSCILLATOR

One of the most extensively studied examples of deterministic chaos is the periodically forced Duffing oscillator[11]

$$\frac{d^2x}{dt^2} = -\delta \frac{dx}{dt} + x - x^3 + \gamma \cos \omega_0 t \tag{5}$$

As is well known, for certain ranges of values of γ, ω_0, and δ the additive forcing term $\gamma \cos \omega_0 t$, hereafter referred to as *primary forcing*, generates a chaotic attractor reflected by aperiodic jumps between the two stable fixed points $x_\pm = \pm 1$ of the unperturbed system. The third fixed point $x_0 = 0$ in the absence of the forcing behaves as a saddle, whose stable and unstable manifolds play an important role in the structure of the chaotic attractor.

Figure 1a depicts the phase space portrait of the system for $\delta = 0.15$, $\gamma = 0.30$, and $\omega_0 = 1$. In contrast to the Lorenz model, another classical example of deterministic chaos, where the system spends most of its time around zero, it appears here that the system spends most of its time around the states x_+ and x_-. This should make the Duffing model a good example of bimodal chaos. Figure 1b provides the implementation of this conjecture on the histogram $P(x)$ of the values of the variable x. Notice, however, that despite the clear-cut difference between the probabilities $P(\pm 1)$ and $P(0)$, the bimodality is much less pronounced than in a stochastic bistable system subject to weak noise. The main reason behind this difference is that in a

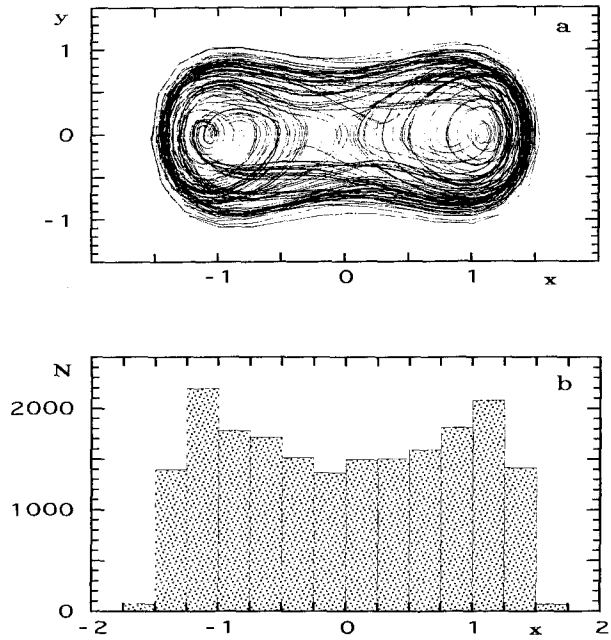

Fig. 1. (a) Phase portrait and (b) histogram of the variable x for the periodically forced Duffing oscillator, Eq. (5). Parameter values: $\delta = 0.15$, $\gamma = 0.30$, $\omega_0 = 1$. The histogram is drawn on the basis of 20,000 equidistant data points obtained from integration of Eq. (5).

typical chaotic attractor internal variability is macroscopic, comparable to the values of the observables themselves.

Figure 2 depicts the probability distribution of residence times in the right part of phase space ($x > 0$). We see that, instead of a smooth exponential-like distribution characteristic of a Markov process one obtains a sequence of discrete peaks centered at $\tau \approx 4$, 9, 15, and 21. This property is to be traced back to the deterministic origin of the system, as a result of which the jumps between the two parts of phase space occur at preferred times. As it turns out, the mean transition time is $\bar{\tau} \approx 8.2$, the dispersion around this mean being of comparable value. Notice that none of these times is related in a simple manner to the forcing period, $T_0 = 2\pi$.

Although a quantitative modeling of the bimodality and the residence time distribution is not available, the following qualitative interpretation can be advanced. One assimilates the system to an overdamped double-well system, the effective potential being (up to a constant)

$$U = -\frac{x^2}{2} + \frac{x^4}{4} \tag{6a}$$

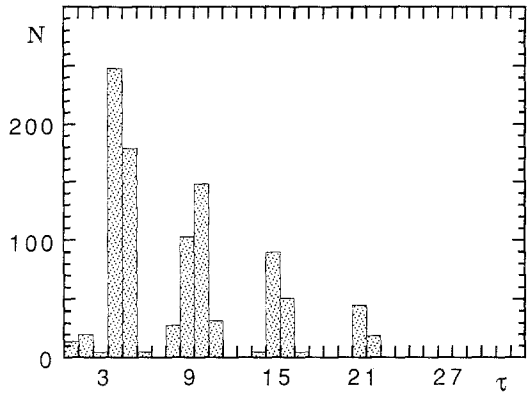

Fig. 2. Probability distribution of residence times of the x variable in the region $x>0$, obtained on the basis of 1000 transitions across the boundary $x=0$. Parameter values as in Fig. 1.

The extrema of this potential are $x_{\pm}=\pm 1$ (minima) and $x_0=0$ (maximum), the potential barrier being $\Delta U_{\pm}=1/4$. Chaos is causing transitions between the two wells at $x_{\pm}$ and is assimilated to an effective noise. Typically this noise is a complex, highly correlated process, but for the purposes of qualitative understanding we assimilate it to a Gaussian white process. We can estimate the variance D_{eff} of this effective noise by the relation

$$P_{\max}/P_{\min} \approx \exp(\Delta U/D_{\text{eff}}) \tag{6b}$$

From Fig. 1b, $P_{\max}/P_{\min}\approx 1.5$, yielding $D_{\text{eff}}\approx 0.5$. This gives a Kramers time

$$\tau_{\text{Kr}} \approx 2\pi\,|U''(1)\,U''(0)|^{-1/2}\,e^{\Delta U/D_{\text{eff}}} \approx 6.7 \tag{6c}$$

which is reasonably close to the simulation result of $\bar{\tau}\approx 8.2$, considering the simplicity of the model.

3. RESPONSE TO A SECONDARY PERIODIC FORCING

We now submit the periodically forced Duffing oscillator, Eq. (5), to a *secondary* periodic forcing in the form of an additive contribution $\varepsilon\cos\omega t$, $\varepsilon\ll\gamma$.

Figure 3 depicts the effect of this perturbation on the residence time distribution. More specifically, it shows how the probability mass around the principal peak of Fig. 2 ($3\leqslant\tau\leqslant 5$) varies with the forcing period. A

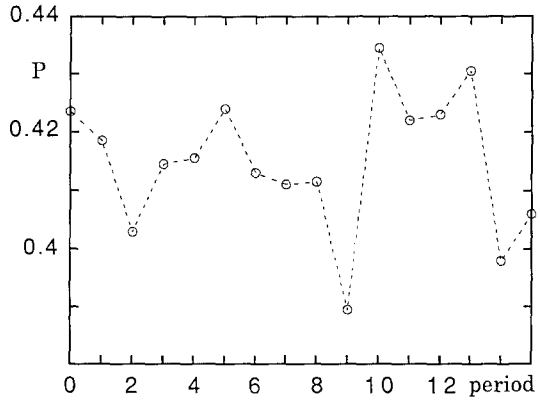

Fig. 3. Dependence of the probability mass P around the principal peak of Fig. 2 on the period T of a secondary forcing $\varepsilon \cos \omega t$ acting on Eq. (5). $\varepsilon = 0.001$ and other parameter values as in Fig. 1. Notice the enhancement of the response at $T = 9$ and $T = 14$.

strong response (of more than 5% for a forcing amplitude of 0.001) is observed at a forcing period around $T = 9$ and, to a lesser extent, at a period around $T = 14$. On the other hand, no clear-cut signature of the secondary forcing on the power spectrum or the signal-to-noise ratio (SNR) can be identified.

Figure 4 illustrates the effect of the secondary forcing of $T = 9$ on the residence time distribution in the $x > 0$ region. We see that the forcing induces, indeed, a substantial reshuffling of the residence time distribution

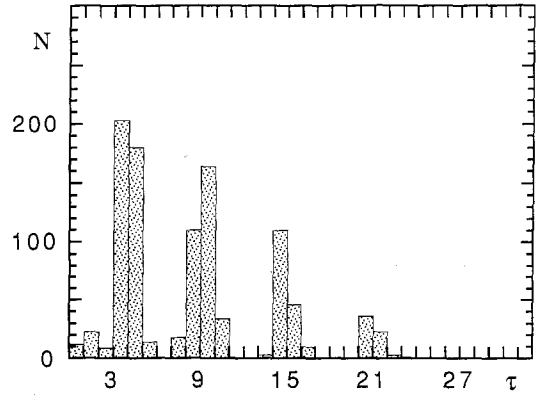

Fig. 4. Probability distribution of residence times of the x variable in the region $x > 0$ for the periodically driven Duffing oscillator in the presence of a secondary forcing of period $T = 9$. Parameter values as in Fig. 3.

reflected by a depression of the dominant peak, an enhancement of the secondary one, and a drift of the mean residence time to a higher value.

Let us outline a qualitative interpretation of these results. First, the absence of signature of the forcing in the SNR can be understood on the basis of ref. 3, since for small perturbation amplitude ε the SNR reduces to

$$\mathrm{SNR} \approx \sqrt{2}\,\varepsilon^2 \frac{1}{4D_{\mathrm{eff}}^2} e^{-\Delta U/D_{\mathrm{eff}}} \approx \varepsilon^2 \cdot [\text{terms of } O(1)] \tag{7}$$

which is very small indeed for $\varepsilon = 10^{-3}$ or so. On the other hand, the enhancement in linear response given by Eq. (4) leads to an effective forcing amplitude

$$\varepsilon_{\mathrm{eff}} = \frac{\varepsilon}{D_{\mathrm{eff}}} \frac{\lambda_1}{\lambda_1^2 + \omega^2} \approx \frac{\varepsilon}{D_{\mathrm{eff}}} \frac{2\pi}{\sqrt{2}} \exp\left(\frac{\Delta U}{D_{\mathrm{eff}}}\right) \approx 10\varepsilon \tag{8}$$

showing that nontrivial effects can indeed be expected.

We now turn to the period dependence of the response at the level of the residence time distribution. A first comment to be made is that this type of response does not fully fit the classical stochastic resonance setting since it does not show a monotonic enhancement for increasing periods, but, rather, an enhanced sensitivity to preferred periods. This is closer to traditional resonance. On inspecting Fig. 2 one recognizes that the forcing periods leading to maximal sensitivity correspond in fact to the second (and, to a lesser extent, the third) largest peak of the residence time distribution of the unperturbed system. One can argue, then, in the spirit of ref. 12, that statistically speaking, the forcing facilitates exit at larger values of τ since it affects coherently the probability mass that is bound to exit at $\tau = 9$ and, to a lesser extent (once every two exits), the one to exit at the primary peak around $\tau \approx 4$.

4. BIMODAL CHAOS IN A ONE-DIMENSIONAL INTERMITTENT MAP

As a second example of bimodal chaos we consider a family of piecewise linear maps defined by (see Fig. 5)[13]

$$\begin{aligned} f(x) &= f_1(x) && 0 \leqslant x \leqslant 1/2 \\ &= 1 - f_1(1-x) && 1/2 < x \leqslant 1 \end{aligned} \tag{9a}$$

with

$$\begin{aligned} &f_1(0) = 0, && f_1(1/2) = 1 \\ &f_1(x) = (1+\delta)\,x, && 0 \leqslant x < a < 1/2, \quad \delta \ll 1 \end{aligned} \tag{9b}$$

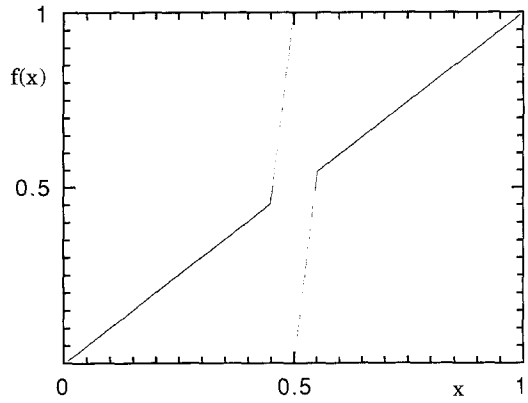

Fig. 5. The map defined by Eqs. (9a)–(9b) for $\delta = 0.01$, $a = 0.4481$. The figure is obtained on the basis of 20,000 data points.

The system exhibits a small-scale "laminar" motion in the regions where the slope is close to unity, followed by a number of "turbulent" bursts and subsequent reinjections back to either of the laminar regions. On these grounds the invariant probability distribution of the x variable is expected to show two pronounced peaks located in these regions. Figure 6, drawn for the parameter values $\delta = 0.01$, $a = 0.4481$, shows that this is indeed the case. Actually, for these parameter values the angular point a is mapped on $x = 1/2$ after exactly two iterations. There exists, then, a 4-cell Markov partition defined by $x = 0$, $f(a)$, $1/2$, $f(1-a)$, 1 on which the dynamics is mapped onto a first-order Markov process governed by a time-

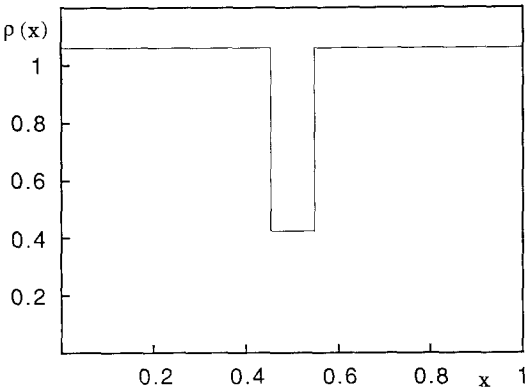

Fig. 6. Invariant probability density of map (9a)–(9b) for the parameter values of Fig. 5. Notice the piecewise constant character of the density, due to the existence of an exact Markov partition.

independent stochastic matrix.[7,8] The eigenvalues of this transition matrix are given by $\lambda_1 = 0.0848$, $\lambda_2 = -0.0863$, $\lambda_3 = 0.9818$, and $\lambda_4 = 1.0000$. The eigenvector corresponding to λ_4 is the invariant state of the system as given, precisely, by Fig. 6, whereas time-dependent properties are dominated by the next largest eigenvalue λ_3. Much as in the Kramers problem, the relevant time scale, given by $1/|\ln \lambda_3| \approx 54.4$, is indeed long. Detailed calculation shows that it is controlled by $1/\delta$, δ being the deviation from slope one in the laminar region. We see that the system at hand possesses an inherent sensitivity measured by a "susceptibility factor" of the order of $1/\delta$ or of $1/|\ln \lambda_3|$. These properties, established analyticaly thanks to the existence of a Markov partition, are expected to hold true for other parameter values provided that the deviation δ from slope one in the laminar region remains small. Independently of any Markov partition, for maps which are symmetric about $(1/2, 1/2)$ one can also show[13] that densities initially symmetric about $x = 1/2$ remain so in their subsequent evolution. Furthermore, on the basis of the Lasota–Yorke theorem,[14] f possesses a smooth invariant probability measure.

Figure 7 depicts the numerically simulated probability distribution of residence times in the part of the phase space given by $f(1-a) < x < 1$. The difference with Fig. 2 is striking, the picture being now much closer to the one corresponding to a noise-driven system. This is due to the existence of the Markov partition and, particularly, the choice of $f(1-a)$ as the exit point of the trajectory.

A qualitative interpretation of Fig. 7 may be advanced on the basis of the idea that the distribution of residence times is dominated by the

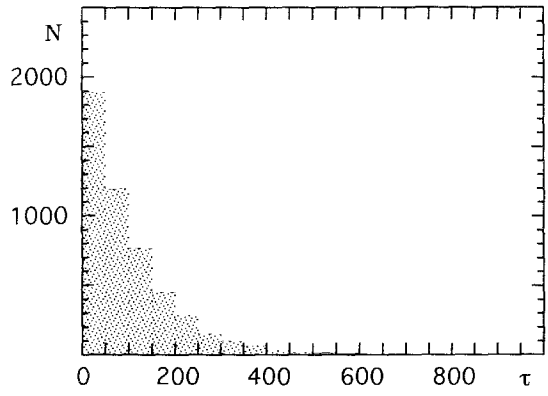

Fig. 7. Probability distribution of residence times of the system of (9a)–(9b) in the region $f(1-a) < x < 1$, obtained on the basis of 5000 transitions across the boundary $f(1-a)$. Parameter values as in Fig. 6.

behavior in the laminar region. To be specific, choosing the region $0 < x < a$, one has from (9a)

$$x_{n+1} = (1 + \delta)\, x_n$$

or, subtracting x_n on both sides and performing the limit of continuous time in the spirit of ref. 15,

$$\frac{dx}{dt} = \delta x$$

Integrating t between $t = 0$ and $t = \tau$ (the residence time) and x between x_0 and a (the exit point), one finds

$$x_0 = ae^{-\delta\tau} \tag{10}$$

On the other hand, by virtue of conservation of probability,

$$\rho(\tau) = \tilde{\rho}(x_0) \left| \frac{dx_0}{d\tau} \right|$$

where $\tilde{\rho}(x_0)$ is the probability density of x_0. Utilizing (10) and assuming uniformly distributed initial conditions x_0 in the interval $0 < x < a$ $[\tilde{\rho}(x_0) = 1/a]$, one finds

$$\rho(\tau) = \delta e^{-\delta\tau} \tag{11}$$

which looks qualitatively like Fig. 7 and predicts an average value $\bar{\tau} = 1/\delta$. For the parameter value adopted here, $\delta = 0.01$, this gives $\bar{\tau} = 100$, in good agreement with the value $\bar{\tau} \approx 102$ deduced from the numerical simulation.

5. THE PERIODICALLY FORCED INTERMITTENT MAP

We now consider the effect of a weak external periodic forcing of zero mean on the system studied in the preceding section. In order to remain within the unit interval, we first choose a multiplicative forcing amounting to a modulation of the slope in the map [Eqs. (9a)–(9b)] by a factor of $\varepsilon = 0.001$, in the form of a square pulse of period T.

Figure 8 summarizes a first series of results of the numerical simulations, in the form of the dependence of the mean residence time on the forcing frequency (broken line). We see that the response is enhanced as the frequency decreases, much as in classical stochastic resonance, the maximum difference as compared to the unforced system being about 5%. This corresponds to an amplification factor of 50, coinciding with the

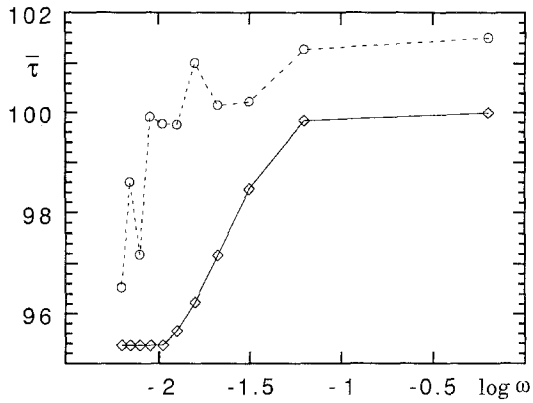

Fig. 8. Response of the map defined by (9a)–(9b) to a multiplicative periodic forcing in the form of a square pulse of zero mean. The figure represents the dependence of the mean residence time versus the forcing frequency. The broken line refers to the result of direct numerical simulation of the system [5000 transitions across the boundary $f(1-a)$] and the full line is drawn on the basis of the analytical formula (13). Forcing amplitude $\varepsilon = 0.001$, other parameters are as in Fig. 6.

inverse of the logarithm of the system's dominant eigenvalue as discussed in the preceding section and in agreement with the general setting of Eq. (4).

A natural qualitative interpretation of these results can be advanced along the lines of Eqs. (10)–(11). We focus on the laminar region, take the continuous-time limit, and choose for simplicity a sinusoidal forcing. Equation (10) is then replaced by

$$x_0 = a \exp\left[-\left(\delta\tau - \frac{\varepsilon}{\omega} \cos \omega\tau \right) \right] \tag{12}$$

leading to

$$\rho(\tau) = \delta \left(1 + \frac{\varepsilon}{\delta} \sin \omega\tau \right) \exp\left(-\frac{\varepsilon}{\omega} \right) \exp\left[-\left(\delta\tau - \frac{\varepsilon}{\omega} \cos \omega\tau \right) \right] \tag{13}$$

This function has the general shape of Fig. 7 and predicts a frequency dependence of the mean residence time given by the continuous line of Fig. 8. The agreement with the result of the direct numerical simulation is satisfactory, considering the simplicity of the arguments leading to Eq. (13).

The shape of the numerically simulated residence time distribution itself is qualitatively similar to that of the unperturbed system, Fig. 7. This is presumably due to the fact that the Markov partition identified in Section 4 still controls the main properties of residence time statistics.

As in the perturbed Duffing oscillator, no clear-cut signature of the forcing appears at the level of power spectrum. The evaluation of the Lyapunov exponent, performed in order to check whether the forced system continuously remains in the chaotic regime, shows no noticeable sensitivity with respect to the forcing parameters.

We finally turn to the response of the system to an additive periodic forcing in the form of a square pulse of zero mean. It is easily checked that the presence of a strictly additive perturbation of this kind in the right-hand side of Eqs. (9a)–(9b) entails that the system is no longer necessarily confined in the unit interval. We therefore introduce periodic boundary conditions, stipulating that if at a certain iteration the representative point is found to be in the region $x<0$ or $x>1$, it is reinjected, respectively, at the points $1+x$ and $x-1$ of the unit interval.

Figure 9 summarizes the dependence of the mean residence times on the forcing frequency. We notice that to obtain this result one counts as transitions from the region $f(1-a)<x<1$ to the region $0<x<f(1-a)$ only those events in which the boundary $f(1-a)$ is crossed: in other words, "transitions" arising from the reinjection process associated with the periodic boundary conditions are discarded. The general trend is the same as in Fig. 8 in the sense that the response is enhanced as the frequency decreases, but, quantitatively speaking, for the same forcing amplitude the response is now much stronger. There is a systematic drift toward lower values of residence times, a trend confirmed by the explicit computation of the residence time distribution as depicted in Fig. 10. This can be under-

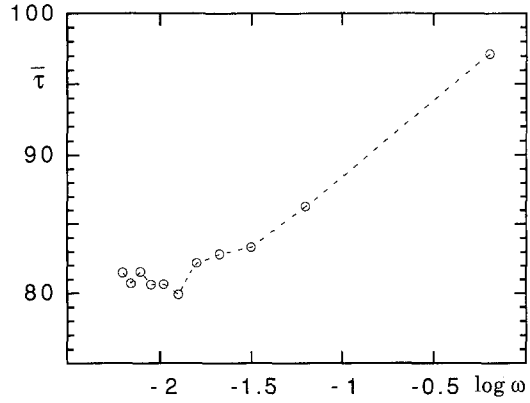

Fig. 9. Response of the map of (9a)–(9b), now subjected to periodic boundary conditions, to an additive periodic forcing in the form of a square pulse of zero mean. The figure represents the dependence of the mean residence time versus the forcing frequency. Parameter values as in Fig. 8.

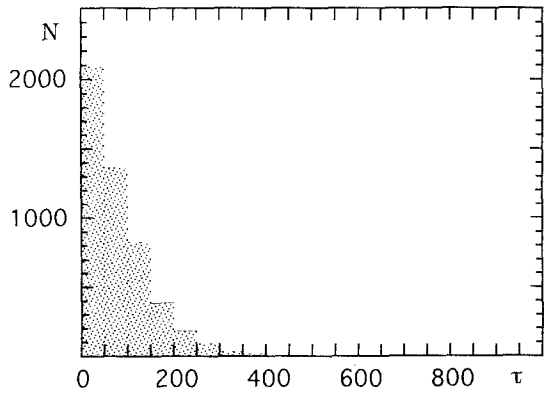

Fig. 10. Probability distribution of residence times of the periodically forced system of Fig. 9 drawn for a forcing period $T=500$ on the basis of 5000 transitions across the boundary $f(1-a)$.

stood by the following simple argument. In a typical event associated with a long residence time the system starts near $x=0$ or $x=1$. In a thin band of width ε near these points the system will either be subjected to a negative (positive) forcing and be brought out of the unit interval, in which case the event is discarded, or it will experience a positive (negative) forcing action, in which case its residence time will be decreased.

One can construct analytically the residence time distribution in the purely additive case as well. Arguing as in Eqs. (12)–(13), one now obtains

$$\rho(\tau)=\frac{1}{a+\varepsilon\delta/(\omega^2+\delta^2)}\frac{-d}{d\tau}e^{-\delta\tau}\left[a-\frac{\varepsilon}{\omega^2+\delta^2}(\omega\sin\omega\tau-\delta\cos\omega\tau)\right] \tag{14}$$

The computation of mean transition times gives the same qualitative behavior as in Fig. 9, but, quantitatively speaking, for a given frequency value the corresponding curve is systematically shifted upward by an amount of 5–10 time units. This quantitative discrepancy should be attributed to the fact that Eq. (14) discards the reinjection process associated with the periodic boundary conditions.

6. DISCUSSION

In this paper the response of chaotic dynamical systems exhibiting bimodality toward weak external periodic perturbations has been studied on two examples: the periodically forced Duffing oscillator and a one-dimensional map showing intermittent-like behavior. It was found that in certain parameter ranges these systems present an enhanced sensitivity to

the periodic perturbation. The mechanism underlying this sensitivity is reminiscent of stochastic resonance, with the major difference that the presence of noise is not required, since deterministic chaos generates its own "effective" noise.

The central property on which sensitivity was tested was the residence time statistics on certain attractor regions, whose boundaries were related to the dynamics in a natural manner. Ordinarily, this property is not considered in chaos theory. Our study shows that it captures a number of interesting features of the underlying system and deserves further consideration. More traditional properties considered in chaos theory such as power spectra appear to be practically insensitive in the limit of weak perturbation amplitudes.

Although our analysis was carried out on two specific examples, the conclusions reached are likely to be more general. Indeed, these examples are generic illustrations of whole classes of dynamical systems capable of giving rise to bimodal chaos.

Finally, throughout our study it was verified that the perturbed system does not undergo a change of regime under the action of the forcing, as was the case in recent work on the suppression of chaos in periodically driven systems.[16–18] In other words, the system remains on a single attractor, which is continuously deformed under the action of the perturbation. This is a necessary condition for studying response properties and for establishing meaningful analogies with classical stochastic resonance.

ACKNOWLEDGMENTS

This work is supported by the Pôles d'Attraction Interuniversitaires Program of the Belgian Government and by the Commission of the European Communities under contract SC1*-CT91-0697 (TSTS) and S/SCI*-900592.

REFERENCES

1. C. Nicolis, *Tellus* **34**:1 (1982).
2. R. Benzi, G. Parisi, A. Sutera, and A. Vulpiani, *Tellus* **34**:10 (1982).
3. B. McNamara and K. Wiesenfeld, *Phys. Rev. A* **39**:4854 (1989).
4. Gang Hu, C. Nicolis, and G. Nicolis, *Phys. Rev. A* **42**:2030 (1990).
5. C. Nicolis, G. Nicolis, and Gang Hu, *Phys. Lett. A* **151**:139 (1990).
6. C. Presilla, F. Marchesoni, and L. Gammaitoni, *Phys. Rev. A* **40**:2105 (1989).
7. G. Nicolis and C. Nicolis, *Phys. Rev. A* **38**:427 (1988).
8. G. Nicolis, Y. Piasecki, and D. McKernan, Toward a Probabilistic Description of Deterministic Chaos, in *From Phase Transitions to Chaos*, G. Györgyi et al., eds. (World Scientific, Singapore, 1992).
9. C. Nicolis and G. Nicolis, *Phys. Rev. A* **34**:2384 (1986).

10. K. Takeyama, *Prog. Theor. Phys.* **60**:613 (1978).
11. J. Guckenheimer and Ph. Holmes, *Nonlinear Oscillations, Dynamical Systems and Bifurcations of Vector Fields* (Springer, Berlin, 1983).
12. T. Zhou, F. Moss, and P. Jung, *Phys. Rev. A* **42**:3161 (1990).
13. D. McKernan and G. Nicolis, Effect of periodic perturbations on an intermittent map, to be published.
14. A. Lasota and J. Yorke, *Trans. Am. Math. Soc.* **186**:481 (1973).
15. Y. Pomeau and P. Manneville, *Commun. Math. Phys.* **74**:189 (1980).
16. L. Fronzoni, M. Giocondo, and M. Pettini, *Phys. Rev. A* **43**:6483 (1991).
17. Y. Braiman and I. Goldhirsch, *Phys. Rev. Lett.* **66**:2545 (1991).
18. D. Ray, *Phys. Rev. A* **42**:5975 (1990).